

Performance Evaluation of Moment Resisting Frames with SCWB and WCSB Configurations using Performance-based Seismic Procedures

Zameer Ahmed, PG Student, Department of Civil Engineering, MGM's College of Engineering, Nanded, Maharashtra, India. zameerahmed143@gmail.com

Mohd. Zameeruddin, Associate Professor, Department of Civil Engineering, Nanded, Maharashtra, India. md_zameeruddin@mngmcen.ac.in

Abstract - In the earthquake resistant design, reinforced concrete sections are designed to carry the gravity and inertia loads within the predefined serviceability limits. The performance of structure under seismic events depends on the size and layout of beam and columns. In the past, several studies were conducted on reinforced concrete structure with both strong column weak beams (SCWB) and weak column strong beams (WCSB) to evaluate the capacity subjected to seismic loads. Also, some studies have been performed on layout of such cases of beams within the plan. In this study attempt has been made to evaluate the performance of moment resisting frames with different configurations of SCWB and WCSB under the performance-based seismic design framework. A parametric study on engineering demand parameters such as modal time period, modal frequencies, storey displacements, inter-storey drift and base shear has been carried out. The results obtained from this parametric study helps to find out the efficacy of the frames integrated with the collapse mechanism and performance levels defined in performance-based design framework. This parametric study provides an easy way of benchmarking the performance of a structure, which may be used in obtaining various design alternatives.

Keywords — Strong column-weak beam, weak column-strong beam, nonlinear static pushover analysis, modal time period and frequency, base shear, storey displacement, inter-storey drift.

I. INTRODUCTION

The earthquake resistance design methodologies defined in the relevant codes are force-based [1]. The structure which was designed using force-based design procedure, when subjected to the seismic loads show poor performance and sustained minor or major damages, in extreme events they were collapsed [2, 3].

MRFs are used as part of seismic force-resisting systems in buildings that are designed to resist earthquakes. Beams, columns, and beam-column joints in MRF frames are proportioned and detailed to resist flexural, axial, and shearing actions, resulted from the lateral sway during strong earthquakes. Special proportioning and ductile detailing makes the MRF capable of resisting strong earthquake without significant loss of stiffness or strength. In current usage, the MRF are capable of resisting at least 25 % of the design seismic forces, while the total seismic resistance is provided by the combination of the moment frame and the shear walls or braced frames in proportion with their relative stiffness's [4].

The collapse mechanism of MRF depends on the capacity of a structural member. Either the lines of resistance will be governed by the beam failure envelope or

column failure envelope. To understand these effects it's needed to evaluate the performance of MRF with Strong Column Weak Beam (SCWB) or Weak Column Strong Beam (WCSB) structural assemblage. In this study, we have evaluated the performance of MRF with SCWB and WCSB configurations. Also, the performance of MRF for alternate layout of beams such as Strong-Weak-Strong (SWS) and Weak-Strong-Weak (WSW) has been studied.

Performance-based seismic design (PBSD) has emerged as the best alternative over the force-based design procedures. PBSD is a generalized design philosophy in which design criteria are expressed in terms of achieving stated performance objectives when the structure is subjected to the stated levels of seismic hazard [5]. PBSD defines various performance levels based on damages sustained by the structural and non-structural components in a seismic event. Namely, Operational level (OP), Immediate Occupancy level (IO), Life-safety range (LS), Collapse prevention (CP) and Collapse (C) identified on the basis of drift. These performances are evaluated at global level and local level. For the global performance level inter-storey drift and storey displacements are used. Wherein; for the local performance level assessment the curvature or

rotation of reinforced concrete members is used. This classification helps the designer to evaluate the nonlinear behavior of structure. PBSD has recommended performance evaluation procedures such as the Capacity Spectrum Method (CSM) and Displacement Coefficient Method (DCM).

In this study, the performance of MRF with SCWB, WCSB, SWS and WSW geometric layout has been evaluated. The nonlinear responses of the MRF have been obtained by performing the nonlinear static analysis (Pushover, POA) for displacement-controlled. The lateral load pattern used for analysis is obtained in accordance to the guidelines of IS 1893. The engineering demand parameters resulting from the POA are used to evaluate the performance of example MRF. The analysis procedure described in this study will help the designer to optimize the structural assemblage, best suited for giving a set of seismic hazard.

Strong Column Weak Beam (SCWB)

To achieve the SCWB hierarchy in MRF, the stiffness of column shall be more than the beam. For the failure mechanism of MRFs, the beam-sway mechanism (i.e. with plastic hinges forming first at beam ends) is preferred to the story-sway mechanism (i.e. with plastic hinges forming first at column ends), as the former generally lead to better seismic performance representing local failure or a sign of failure not a complete collapse. The beam-sway mechanism results in higher energy dissipation capacity with less demand of ductility on structural components, leading to a more uniform distribution of the story drift and higher resistance to seismic loads at the structural level [6].

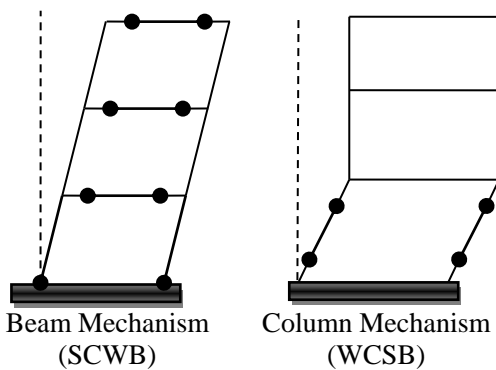


Fig. 1: Possible failure mechanism of MRF

In SCWB, the sum of the flexural capacities of the columns at a joint ($\sum M_c$) is required to be larger than that of the beams framing into the joint ($\sum M_B$), as expressed in the following equation

$$\sum M_c = \gamma \sum M_B \tag{1}$$

Where γ is called the column-to-beam flexural strength ratio and should be equal to 1.4 [7]. Table 1 shows the γ value defined in various international codes.

Weak Column Strong Beam (WCSB)

When the relationship expressed in Eq. 1 is overruled the resulting assembly represents WCSB. WCSB results in column failure mechanism, in which failure, concentration

occurs at single storey leading to the catastrophic collapse of whole structure questioning the stability. Fig 1, illustrates the difference between SCWB and WCSB mechanism.

Table 1: Values of γ defined in relevant codes

Relevant codes	γ value
ACI 318 14: 2014	1.2
Eurocode 8 CEN: 2004	1.3
NZS 310:2006	1.3
IS 13920:2016	1.4

In past a study conducted on MRFs has proposed procedures to arrive at the required strength at a joint [8] and showed that SCWB design criterion leads to a significant reduction in collapse probability, particularly in the case of mid-rise buildings [9]. The relative importance of Strong Column-Weak Beam (SCWB) design concept in comparison to other code-prescribed details for a reinforced concrete MRF was verified by experimental study conducted on a scaled model of the MRF [10]. Some comparative studies have been conducted in past on SCWB and WCSB to understand the efficacy of the structural framing system under inelastic excursions [11].

In the present study, we have attempted to evaluate the performance of example MRFs which were designed in accordance to IS 1893 and IS 13920 guidelines. For this purpose four example MRFs representing SCWB, WCSB, SWS and WSW configurations are subjected to the POA and parametric study is carried out to evaluate efficacy of MRFs under seismic loads.

II. EXAMPLE MOMENT RESISTING FRAMES

In this study, we conducted a performance-based seismic evaluation of MRFs representing a general trend of constructions of low-rise structures adopted in India. Fig. 2 depicts the typical layout of the example MRFs. These MRFs represent a regular office building in the seismic zone V, as per IS 1893, on a medium soil type. The height of each story of the model was assumed as 3 m, and the beam spanned 3 m. The spacing between the frames was 3 m. The characteristics of these MRFs are presented in Table 2.

For the analysis, dead loads, live (imposed) loads, and seismic loads were considered as per IS 875 (Parts 1 and 2) [12-13] and IS 1893, respectively. These MRFs are subjected to a mean dead load of 11.67 kN/m² (inclusive of the finishes loads) and a mean live load of 3 kN/m² for all floors. The RC design of these MRFs was based on IS 456 [14] guidelines. The ductile (seismic) detailing of the RC section was based on IS 13920 provisions. The material properties considered in the design are presented in Table 3.

The structural design of the example MRFs is presented in Table 4. The structural design of the example MRFs is not a unique solution available for the calculated demand. Based on the same demand, different designers may select different solutions. The RC member sizes were selected by following a common practice adopted by engineers. All the columns and beams in a selected story are identical in cross section. The column remained uniform in cross section up to three stories, depending on the height of the building.

III. NONLINEAR STATIC ANALYSIS (PUSHOVER ANALYSIS)

We performed displacement-controlled POA on the example MRFs by using SAP 2000 V 20.0 [15]. The target displacement used for each MRF was 4% of the height of the frame [16]. The analysis was conducted in two stages for the following: (i) gravity loads and (ii) predominant lateral loads. In stage I, gravity loads were applied as the distributed element loads on the basis of the yield line theory and concentrated loads from secondary beams. Gravity analysis was performed for full gravity load in a single step (i.e., force-control). The state of the structure in this analysis was saved and was subsequently recalled in stage II. In stage II, lateral loads were applied monotonically in a step by-step nonlinear static analysis. Because the lateral force profile in POA influences the structural response, a set of lateral loads were used.

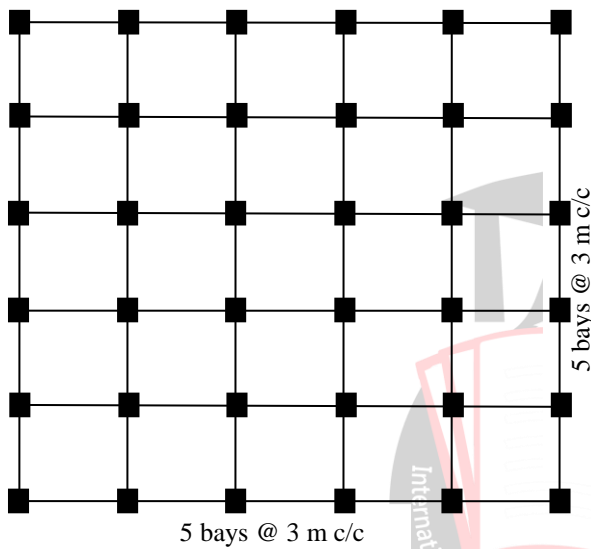


Fig 2 (a): Typical Plan of example MRFs

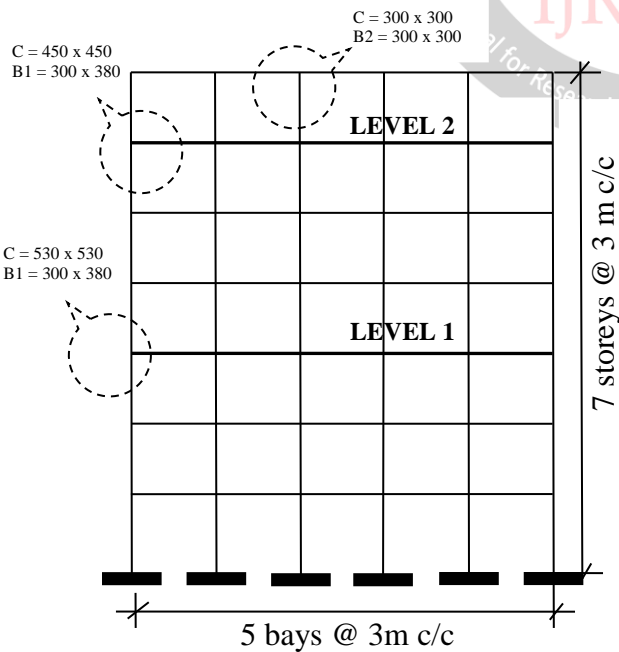


Fig 2 (b): Typical Elevation of SCWB MRFs

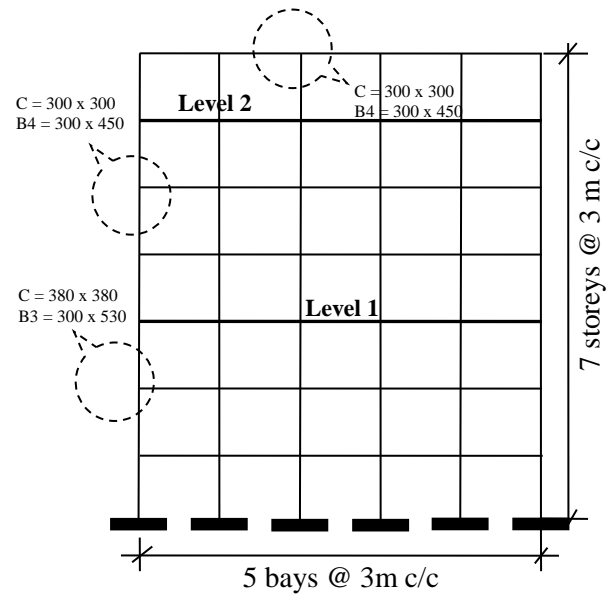


Fig 2 (c): Typical Elevation of WCSB MRFs

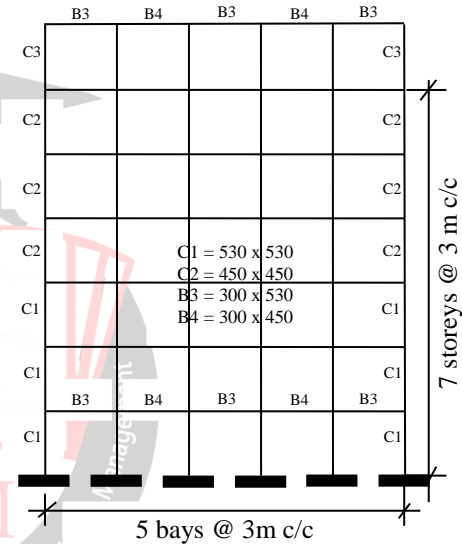


Fig 2 (d): Typical Elevation of SWS MRFs

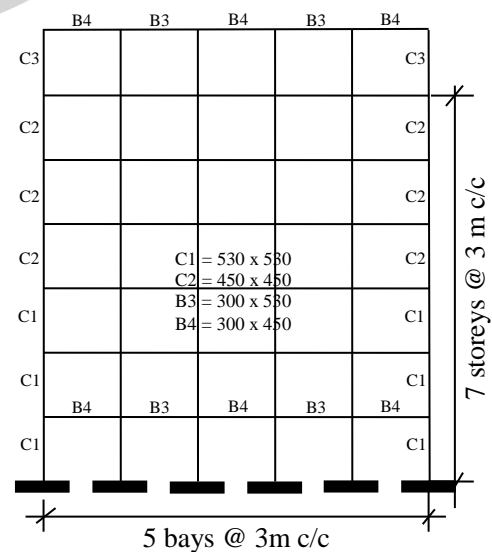


Fig 2 (e): Typical Elevation of WSW MRFs

Table 2: Characteristics of the studied example MRFs

Example MRF	T _d (s)	T _m (s)	S _a	W _i (kN)	V _b (kN)
SCWB	0.735	0.434	2.5	1095.37	98.58
WCSB	0.735	0.448	2.5	908.17	81.73
SWS	0.735	0.345	2.5	1211.66	110.18
WSW	0.735	0.352	2.5	1224.26	109.05

Table 3: Material properties considered in the design of example MRFs

Material property	Concrete M 25 Grade	Steel Fe 415 Grade
Weight per unit volume (kN/m ³)	25	76.97
Mass per unit volume (kN/m ³)	2.548	7.849
Modulus of elasticity (kN/m ²)	25E+06	2E+08
Characteristic strength (MPa)	25000 (for 28 days)	415000 (yield)
Minimum tensile strength (kN/m ²)	-	485800
Expected yield strength (kN/m ²)	-	456500
Expected tensile strength (kN/m ²)	-	533500

Table 4: Design details of RC members of example MRFs

RC Member	Storey Level	Cross-section	Rebar's details (mm ²)
SCWB			
Column (C1)	1-3	530 x 530	2809
Column (C2)	4-6	450 x 450	720
Column (C3)	7	300 x 300	900
Beam (B1)		300 x 380	Top - 600 Bottom - 330
Beam (B2)		300 x 300	Top - 600 Bottom - 300
WCSB			
Column (C1)	1-3	530 x 530	1155
Column (C2)	4-6	450 x 450	720
Column (C3)	7	300 x 300	777
Beam (B1)		300 x 380	Top - 600 Bottom - 400
Beam (B2)		300 x 300	Top - 600 Bottom - 400
SWS			
Column (C1)	1-3	530 x 530	2809
Column (C2)	4-6	450 x 450	2025
Column (C3)	7	300 x 300	900
Beam (B3)		300 x 530	Top - 600 Bottom - 300
Beam (B4)		300 x 450	Top - 600 Bottom - 300
WSW			
Column (C1)	1-3	530 x 530	2809
Column (C2)	4-6	450 x 450	2025
Column (C3)	7	300 x 300	900
Beam (B3)		300 x 530	Top - 600 Bottom - 300
Beam (B4)		300 x 450	Top - 600 Bottom - 300

Table 5: Lateral Loads on the example MRFs

Storey height	Lateral Loads (IS 1893)			
	SCWB	WCSB	SWS	WSW
3	1.203	0.852	1.214	1.207
6	4.811	3.407	4.855	4.827
9	9.884	7.073	10.033	9.968
12	15.045	10.747	16.252	16.132
15	23.508	16.792	25.394	25.206
18	28.449	24.181	31.451	31.167
21	15.684	18.679	20.985	20.542

Three different lateral load cases are applied on example MRFs. (a) Lateral loads as per IS 1893, (b) Lateral loads for uniform distribution of inertia loads, and (c) First mode lateral load distribution. The IS 1893 lateral loads on the example MRFs for POA are presented in Table 5.

The nonlinear behavior of the frames primarily depends on the moment–curvature (M–φ) behavior of its members. The input required for nonlinear modeling in SAP 2000 is the moment–rotation (M–θ) relationship instead of the moment–curvature relationship). To develop the M–θ curve of a default hinge, a stress–strain relationship described in FEMA 356 [17] integrated in the software was used. For an MRF in which lateral loads are predominant, the contra-flexure point typically occurs in the mid span of the members. Many researchers suggested that for a lumped plasticity model, plastic hinge formation at both ends of the member is most suitable for pushover [18–21].

In this study, beams and column elements were modeled as nonlinear frame elements by assigning concentrated M3 and P-M3 plastic hinges, respectively, to both the ends. FEMA 356 guidelines related to modeling parameters and acceptance criteria were adopted. The acceptance criteria for the ultimate rotation capacity, labeled IO, LS, and CP, are illustrated in Fig. 3.

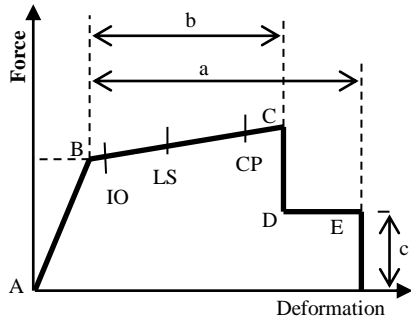
IV. PERFORMANCE ASSESSMENT

The responses of the example MRFs were studied in terms of the fundamental period of vibration, base shear, roof displacement, story displacement, and inter-story drift ratio. The natural period of vibration, evaluated from the empirical equation given in IS 1893 for buildings without infills, is presented in Table 6.

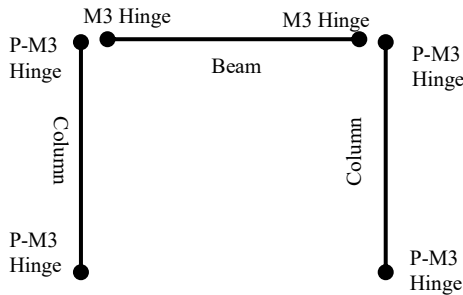
In addition, modal analysis of the MRFs was performed to determine a fundamental period of vibration by using eigenvalues; the results are reported in Table 6. The fundamental period is the first-mode longest modal time period of vibration.

Table 6: Fundamental time period and modal frequencies

Example MRF	T _d (s)	T _m (s)	Modal Frequencies (ω _n) rad/sec
SCWB	0.735	0.434	2.29
WCSB	0.735	0.448	2.23
SWS	0.735	0.345	2.89
WSW	0.735	0.352	2.83



(a) Deformation control (flexure failure)



(b) Location of hinges

Fig. 3: Idealized inelastic force–deformation relationship
The result of POA is presented in the form of a capacity curve, which is typically a plot of rooftop displacement versus base shear. Fig 4 and 5 shows the pushover curve of example MRFs.

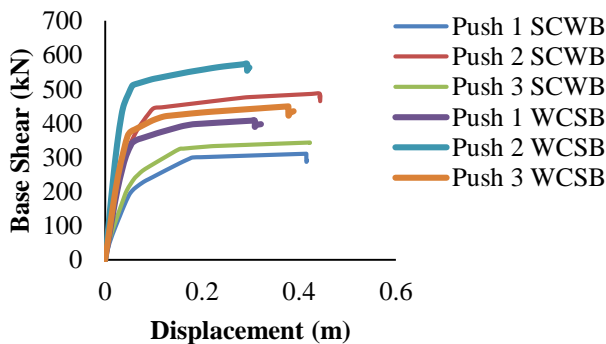


Fig. 4: Pushover Curve of example MRFs with SWS and WSW geometric layout subjected to different lateral load cases

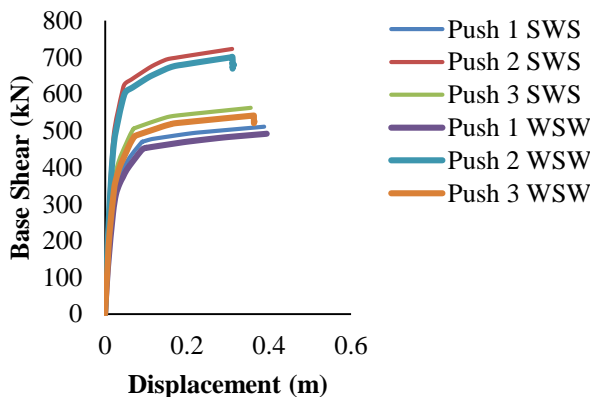


Fig. 5: Pushover Curve of example MRFs with SWS and WSW geometric layout subjected to different lateral load cases

Table 7-8, presents the base shear and the rooftop displacement of MRFs for different load patterns. The obtained results showed that Push 2 load case represents upper bound values and Push 1 Load case represents lower bound values. Whereas Push 3 provides median values. Thus, for optimizing the nonlinear response a set of lateral loads is needed to be applied on MRFs.

Table 7: Nonlinear responses of example MRFs for Capacity Spectrum Method (CSM)

Example MRF	ATC 40 (CSM)		FEMA 440 (CSM)	
	V _p	D _p	V _p	D _p
SCWB				
Push 1	232.87	0.086	245.91	0.103
Push 2	372.12	0.063	410.84	0.081
Push 3	263.13	0.079	279.27	0.098
WCSB				
Push 1	344.01	0.058	347.65	0.061
Push 2	472.89	0.044	480.69	0.047
Push 3	375.50	0.053	377.72	0.056
SWS				
Push 1	403.36	0.047	422.79	0.057
Push 2	558.51	0.032	614.24	0.044
Push 3	445.51	0.044	470.67	0.055
WSW				
Push 1	386.18	0.05	403.02	0.059
Push 2	548.32	0.036	592.29	0.046
Push 3	425.87	0.045	440.55	0.051

Table 8: Nonlinear responses of example MRFs for Displacement Coefficient Method (DCM)

Example MRF	FEMA 356 (DCM)		FEMA 440 (DCM)	
	V _p	D _p	V _p	D _p
SCWB				
Push 1	283.84	0.156	300.19	0.197
Push 2	445.35	0.108	447.76	0.122
Push 3	318.70	0.145	328.62	0.18
WCSB				
Push 1	363.62	0.092	366.92	0.099
Push 2	514.56	0.063	514.14	0.062
Push 3	397.80	0.083	400.74	0.087
SWS				
Push 1	428.85	0.061	452.21	0.077
Push 2	596.68	0.04	626.39	0.048
Push 3	472.79	0.055	500.46	0.067
WSW				
Push 1	418.66	0.069	441.40	0.085
Push 2	590.61	0.046	605.87	0.051
Push 3	452.78	0.056	482.55	0.07

Fig. 6 (a-d) presents the failure mechanism of example MRFs in terms of the plastic hinges. The collapse mechanism envelope represent the yield mechanism of the structure and forms the basis of damage assessment on the

basis of transfer of plastic hinge from one performance level to other performance levels. It also helps in the identification of damage patterns and weak zones both on local levels and global levels.

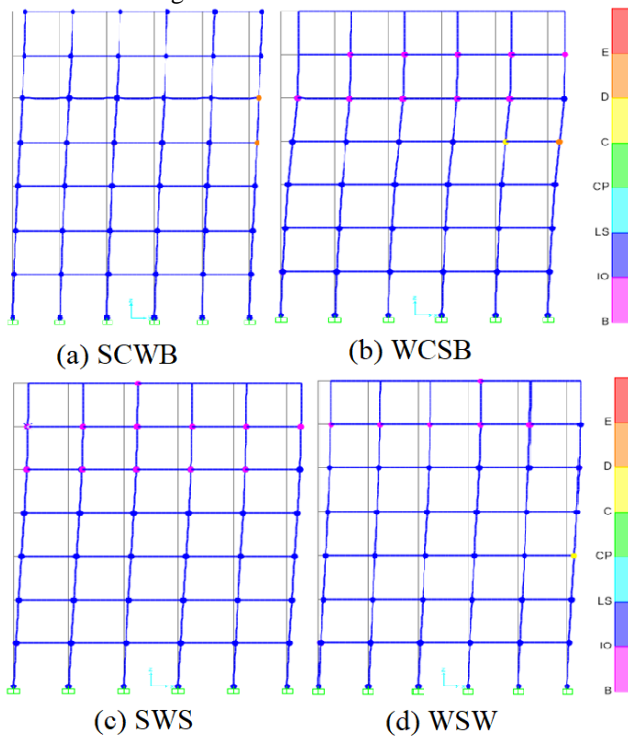


Fig 6: Collapse mechanism of example MRFs for Push 1
The story drift is a useful and simple measure of the overall structural deformation that is routinely examined [5]. Fig. 7 illustrates the story displacements corresponding to different load patterns in the pushover analysis of the example MRFs. The overall interpretations of story displacements provide the following results. Push 2 load case underestimated the story displacements with the increase in the height of the building. In case of WCSB there is fall in ductility of MRF as compared to SCWB MRFs. It may be concluded that WCSB behavior is brittle. It was observed that there is no significant impact of geometric layout on the ductility of the structure.

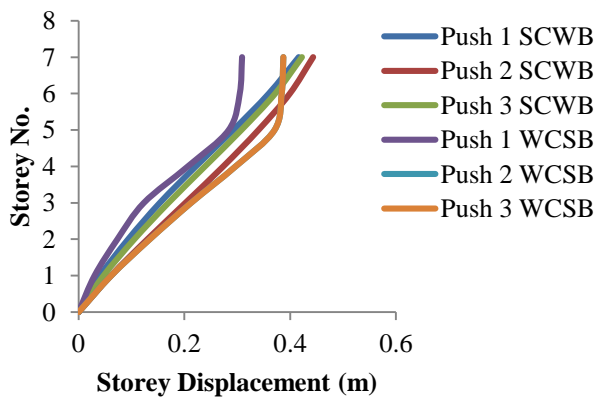


Fig. 7(a): Storey displacements of SCWB and WCSB MRFs

Fig. 8 presents the inter-story displacements of the example MRFs. For a ductile MRF, the inter-story drift is uniform along the height of the structure, but the observed distribution of the inter-story drift ratio along the height of

the building was non-uniform with the increase in the height of the structure. This may be attributed towards an adopted lateral load pattern.

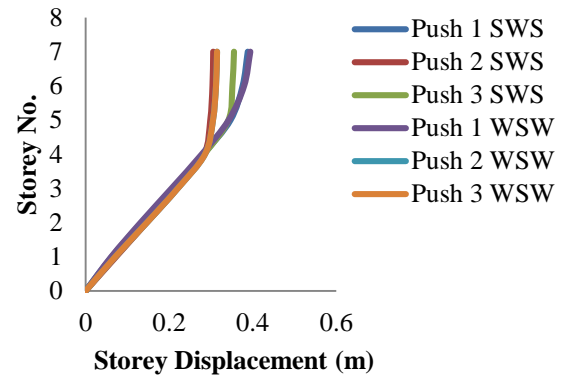


Fig. 7(b): Storey displacements of SWS and WSM MRFs

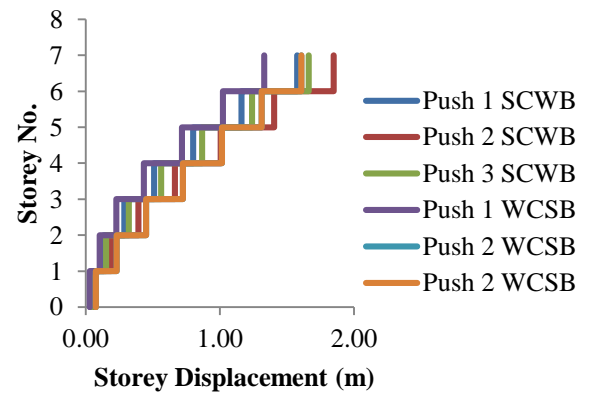


Fig. 8(a): Inter-story drift of SCWB and WCSB MRFs

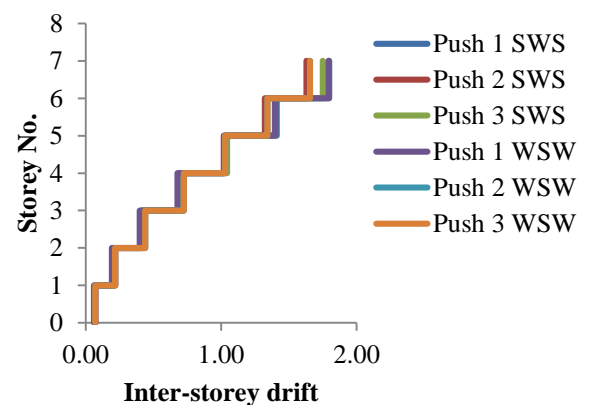


Fig. 8(b): Inter-story drift of SWS and WSM MRFs

Conclusion

The prime focus of the structural engineer is to evaluate the safety of structure during major earthquakes. The present seismic design methodology available in seismic code is force-based where the inelastic behavior of RC structure is taking care through application of modification factors, which misleads towards performance evaluation. PBSD has emerged as the best alternative towards these forces-based methods. In PBSD the performance of a structure is

evaluated in terms of building performance levels which are set in context to drift limits and damage sustained by structural and non-structural components. PBSD provides various performance evaluation procedures like CSM and DCM. These procedures compare the capacity of a structure with imposed demand on the structure. The intersection of capacity spectrum and demand spectrum is called as performance point. The collapse mechanism shows the yielding of RC members in the form of plastic hinges, which can be used to trace the inelastic behavior of the structure. In the present study a parametric study has been carried out using these performance-based evaluation procedures.

The POA carried on example MRFs result in to following concluding remarks;

1. There is considerable difference between the fundamental time period and modal time period. This difference may be attributed towards the geometric configuration of structure and structural components which has been neglected by present seismic code procedures while defining the empirical relations.
2. A set of lateral load pattern was applied on example MRFs. The obtained results revealed that the equivalent lateral load pattern defined in seismic code results in lower bound values of base shear and displacement. Hence a set lateral load pattern is needed for the optimizing the structural response under the lateral loads.
3. The plastic hinge mechanism resulting from a performance based evaluation procedure describes the inelastic excursion through the fall from one performance level to other. This will help designer to keep his structural configuration in a safer zone with minimum associated damages.
4. The deformed shaped of structure in terms of storey and inter-storey displacement describes the efficacy and adequacy of applied lateral load patterns.
5. When the overall performance of various structural system forms like SCWB and WCSB is compared, it may be concluded that WCSB shows brittle failure compared to SCWB.
6. When SWS and WSW geometric layout were compared they showed nearly same results and no clear idea about structural behavior is set up.

The present study is an attempt to understand the behavior of example MRFs with various structural frameworks and geometric layout. The design adopted in this study is not unique, with same loading and cross-section different results may be obtained. This study attempts to identify a performance evaluation procedure for assessment of MRFs and leaves a gray area for future improvements in the state of practice.

ACKNOWLEDGMENT

The authors of this paper acknowledge the research contributions of all the citations under reference and the

support of faculty members and by the Chairman, MGM College of engineering, Nanded, India.

REFERENCES

- [1] IS 1893, *Indian standard for earthquake resistant design of structures (part 1): general provisions and buildings*. Bureau of Indian standards, New Delhi, 2002.
- [2] Ghobarah, A., "Performance-based design in earthquake engineering: state of development," *Engineering. Structures*, 23, pp 878–884, 2001. [https://doi.org/10.1016/s01410296\(01\)00036-0](https://doi.org/10.1016/s01410296(01)00036-0).
- [3] Zameeruddin M., Sangle, K.K., "Review on recent developments in performance-based seismic design of reinforced concrete structures", *Structures*. 6, pp 119 – 133, 2016. <https://doi.org/10.1016/j.istruc.2016.03.001>
- [4] Jack P. Moehle, John D. Hooper and Chris D. Lubke, "Seismic Design of Reinforced Concrete Special Moment Frames: A Guide for Practicing Engineers", NEHRP Seismic Design Technical Brief No. 1, 2008.
- [5] Zameeruddin M., Sangle, K.K., "Performance-based Seismic Assessment of Reinforced Concrete Moment Resisting Frame", *Journal of King Saud University – Engineering Sciences*, 33, pp 153 –165, 2021. <https://doi.org/10.1016/j.jksues.2020.04.005>
- [6] Xuefei Nie, Shishun Zhang, Tao Jiang and Tao Yu, "The strong column–weak beam design philosophy in reinforced concrete frame structures: A literature review", *Advances in Structural Engineering*, 29 (16), pp 1 – 26, 2020. <https://doi.org/10.1177/1369433220933463>
- [7] IS 13920, "Ductile detailing of reinforced concrete structures subjected to seismic force-code of practice", Bureau of Indian standards, New Delhi, 2016.
- [8] A. R. Vijayanarayanan, Rupen Goswami and C. V. R. Murty, "Simple Linear Elastic Static Analysis Procedure to Attain Desired Collapse Mechanism for Moment Resisting Frames", 16th World Conference on Earthquake Engineering, Santiago Chile, 9th to 13th January 2017 Paper No. 1400. <https://www.wcee.nicee.org/wcee/article/16WCEE/WC EE2017-1400.pdf>
- [9] Mitesh Surana, Yogendra Singh and Dominik H. Lang, "Effect of Strong - Column – Weak - Beam design provision on the seismic fragility of RC frame buildings", *International Journal of Advanced Structural Engineering*, 10, pp 131-141, 2018. <https://doi.org/10.1007/s40091-018-0187-z>
- [10] Mohammadreza Vafaeia, Mahmoud Baniahmadi, Sophia C. Alih, "The relative importance of strong column-weak beam design concept in the single-story

- RC frames”, *Engineering Structures*, 185, pp 159-170, 2019. <https://doi.org/10.1016/j.engstruct.2019.01.126>
- [11] Rita Bento and Mário Lopes, “Evaluation of the Need for Weak Beam – Strong Design in Dual Frame-Wall Structures”, 12th World Conference on Earthquake Engineering, Auckland, New Zealand, January 30th to 4th February 2000, Paper No. 0784. <https://www.iitk.ac.in/nicee/wcee/article/0784.pdf>
- [12] IS 875, Code of practice for design loads (other than earthquake) for buildings and structures: part 1 dead loads. Bureau of Indian standards, New Delhi, 1987.
- [13] IS 875, Code of practice for design loads (other than earthquake) for buildings and structures: part 2 imposed loads. Bureau of Indian standards, New Delhi, 1987.
- [14] IS 456, Indian standard plain and reinforced concrete – code of practice (fourth revision). Bureau of Indian standards, New Delhi, 2000.
- [15] Wilson, E.L., Habibullah, A., SAP 2000/NL-push version 20 software, computer and structures, Inc, Berkeley, CA, USA. 2000.
- [16] ATC 40, Seismic evaluation and retrofit of the existing concrete building, Applied Technical Council, Redwood City (CA), 1996.
- [17] FEMA 356, Pre-standard and commentary for seismic rehabilitation of buildings. Federal Emergency Management Agency, Washington (DC), 2000.
- [18] Al-haddad M.S., and Siddiqui, G.H., “Mathematical modeling for cyclic loading of RC beam with relocatable plastic hinge”, *Journal of King Saud University – Engineering Sciences*, 2 (2), pp 213–228, 1990. [https://doi.org/10.1016/S1018-3639\(18\)30615-9](https://doi.org/10.1016/S1018-3639(18)30615-9)
- [19] Akanshu Sharma, K.N., Vaity, G.R., Reddy, K.K., Vaze Ghosh, A.K., Seismic Requalification of RLG Building, Reactor Atomic Research Center, Mumbai, India, 2005
- [20] Mondal, A., Ghosh, S., Reddy, G.R., “Performance-based evaluation of the response reduction factor for ductile RC frames”, *Engineering Structures*, 56, pp1808–1819, 2013. <https://doi.org/10.1016/j.engstruct.2013.07.038>.
- [21] Zameeruddin, M., Sangle, K.K., “Seismic performance evaluation of reinforced concrete frames subjected to seismic loads”, *J. Inst. Eng. India Ser. A* 98, 177–183, 2017. <https://doi.org/10.1007/s40030-017-0196-0>